Research Square

Preprints are preliminary reports that have not undergone peer review.
They should not be considered conclusive, used to inform clinical practice,
or referenced by the media as validated information.

Numerical Methods for Telegraph Equations: A focused review and a variable coefficient benchmark

Amir K Amir

nawrozzmanawani@gmail.com

Hasanuddin University

Systematic Review

Keywords: Telegraph equation, finite differences, temporal convergence, variable coefficients, manufactured solution, discrete energy

Posted Date: November 23rd, 2026

DOI: https://doi.org/10.21203/rs.3.rs-11811881/v1

License: This work is licensed under a Creative Commons Attribution 4.0 International License.
Read Full License

Additional Declarations: The authors declare no competing interests.

Numerical Methods for Telegraph Equations: A focused review and a variable coefficient benchmark

Amir Kamali
Department of Mathematics, Hasanuddin University, Makassar, Indonesia

Abstract

Published numerical studies of the telegraph equation differ in their coefficients, boundary data and error measures, so their reported errors seldom allow a direct comparison. This article reviews 22 primary journal publications and compares two time integrators on a shared one-dimensional benchmark. Reanalysis of four published constant-coefficient examples gave observed refinement orders of 0.971–1.041 for first-order schemes and 1.995–1.999 for second-order schemes. The new benchmark uses the same centred spatial stencil with backward Euler and the trapezoidal rule under constant and smoothly varying coefficients. The trapezoidal rule showed approximately second-order convergence in both the spatial and temporal sweeps. Backward Euler approached first order in time on the finest temporal refinements. In the variable-coefficient case, it gave a smaller error on the coarsest jointly refined grid because spatial and temporal errors partly cancelled. At the finest joint resolution, its error was about 7.6 times the trapezoidal error. Both integrators dissipated the discrete energy in unforced tests. Separate refinement sweeps and a common evaluation time make these comparisons more informative than errors reported on a single grid.

Keywords Telegraph equation, finite differences, temporal convergence, variable coefficients, manufactured solution, discrete energy

1 Introduction

A signal on a transmission line propagates while losing amplitude. The telegraph equation represents both behaviours through a second time derivative and a damping term [2, 22]. Numerical methods must resolve the propagation accurately while reproducing the damping. Stability can keep a computation bounded, but an overly dissipative approximation can still distort the signal.

Köksal [22] surveys the modelling of constant- and variable-coefficient telegraph equations and the numerical methods used to solve them. The present study asks a narrower question. What can the published error tables establish about convergence, and what changes when two methods are run under matched conditions? To address this question, the study compares published refinement data and then runs a benchmark that holds the spatial discretization fixed

while changing the time integrator.

2 Review scope and synthesis

The review builds on a selected set of journal publications identified through web searches using “telegraph equation,” “telegrapher equation,” and related terms for finite differences, differential quadrature, spectral methods and fractional derivatives. The primary set comprises 22 full journal publications from 2008 to 2026 that develop or test a numerical method for a telegraph equation. The existing survey [22] and the related wave-equation article [21] provide context beyond the 22 primary studies. This is a focused, non-exhaustive review. Studies were compared by equation class, boundary conditions, discretization, and the stability or error evidence they report.

Table 1 maps the primary studies to their main discretization families. Akgül and Faraj [21] use first- and second-order finite differences for wave initial–boundary value problems, with MATLAB comparisons to exact solutions. That work is relevant to the undamped wave limit of the classical model, obtained when the damping and reaction terms vanish. Its results do not enter the telegraph-equation error comparisons.

Table 1 Numerical approaches in the primary studies

Approach	What the studies establish	What to match in a comparison
Finite differences [1–5, 10, 23]	Operator and matrix analyses give stability results under specified assumptions. Studies include one-dimensional Dirichlet and mixed data and generalized finite differences in 2D and 3D.	Spatial stencil, time step, boundary treatment and the assumptions of the stability result.
Spline and meshless collocation [6–8]	Thin-plate splines and other radial bases have been tested in 1D or 2D. Cubic B-splines have also been tested on a 1D Neumann problem.	Node locations, basis parameters, boundary enforcement and system conditioning.
Differential quadrature [9, 11–12]	Polynomial, Fourier or B-spline weights approximate derivatives in tests covering Dirichlet and Neumann data and up to three spatial dimensions.	Time integrator, number of unknowns and error measured at common points.
Spectral, wavelet and transform methods [13–17, 24]	Spectral Galerkin and Chebyshev collocation have been tested on smooth problems. Wavelet methods have also been used for nonlinear examples and interface problems.	Regularity, polynomial or wavelet resolution, interface conditions and error norm.
Time-fractional schemes [18–20]	Published approaches include nonlocal boundary data, hybridized discontinuous Galerkin and Laplace–Chebyshev approximation.	Fractional order and convention, boundary and initial data, and evaluation time.

Two distinctions matter in practice. Unconditional stability in the settings covered by Mohanty

[1] and a step-size restriction for the explicit scheme of Ureña et al. [5] concern different discrete problems. Spiteri and Messine [23] compare explicit and implicit schemes under Dirichlet and mixed conditions, illustrating why boundary treatment belongs in the comparison. Smooth spectral tests [13, 14, 16, 17] and interface tests [24] pose different approximation demands. Ranking them by the smallest error reported in each paper would confound method choice with problem difficulty.

3 Published convergence evidence

Only the paired results in Faraj and Modanli [4] and Modanli, Faraj and Ahmed [10] were used for the quantitative reanalysis in Table 2. The two papers report first- and second-order finite-difference schemes on matched grids against exact solutions. The observed order is $\log_2(Ec/Ef)$, where Ec and Ef denote the coarse- and fine-grid maximum errors. Both grid counts are doubled. The papers take the maximum over slightly different time-index ranges, so the ratios are calculated within each example.

Table 2 Published errors and observed orders under joint grid refinement

Source and case	Grid counts	First-order error Coarse / fine	Second-order error Coarse / fine	First-order rate	Second-order rate
[4] Example 1	50 → 100	6.3671×10^{-3} 3.2491×10^{-3}	1.1560×10^{-4} 2.8997×10^{-5}	0.971	1.995
[4] Example 2	50 → 100	4.3329×10^{-2} 2.1858×10^{-2}	1.5960×10^{-4} 4.0048×10^{-5}	0.987	1.995
[10] Table 1	100 → 200	1.8400×10^{-3} 8.9448×10^{-4}	7.5204×10^{-5} 1.8815×10^{-5}	1.041	1.999
[10] Table 2	100 → 200	8.0644×10^{-3} 4.0783×10^{-3}	8.8693×10^{-5} 2.2207×10^{-5}	0.984	1.998

Across these examples, doubling the grid counts roughly halved first-order errors and quartered second-order errors. The later paper [10] derives schemes for a variable-coefficient formulation, but both main error tables use constant-coefficient examples. Its separate variable-coefficient test reports a first-order maximum error of 0.87021 at N = 21 and M = 20. That single run cannot establish a variable-coefficient convergence rate. This motivates independent spatial and temporal sweeps in the following benchmark.

4 Computational benchmark

4.1 Model and manufactured solution

The benchmark solves the non-divergence-form equation

$$u_{tt} + a(x)u_t + bu = q(x)u_{xx} + f(x,t), \quad 0 < x < 1, \qquad 0 < t \le 1. \quad (1)$$

Both cases use homogeneous Dirichlet boundaries and b = 0.75. The constant case uses a = 0.5 and q = 1. The variable case uses a(x) = 0.5 + 0.25x and q(x) = 1 + 0.5x. The exact solution is

$$u(x,t) = e^{-t}\sin(\pi x) + 0.2\cos(3t)\sin(2\pi x). \quad (2)$$

The two spatial modes allow spatial and temporal errors to affect the waveform differently. Initial displacement and velocity come from (2). The forcing is the residual obtained by substituting (2) into (1), namely $f = u^*_{tt} + au^*_t + bu^* - qu^*_{xx}$. This preserves the exact solution in both coefficient cases while testing different operators.

4.2 Discretization and refinement protocol

Let N be the number of spatial intervals, h = 1/N, and Δt the time step. At the interior nodes, D_h is the centred three-point approximation of the second spatial derivative with zero boundary values. Define Q = diag(q), A = diag(a), and $K = bI - QD_h$ using nodal coefficient values. Writing the grid solution as y = (U,V), with V the discrete velocity, gives $\dot{y} = Ly + g$, where L(U,V) = (V, −KU − AV) and g = (0,f).

At each step, the linear system for the two θ-methods is

$$(I - \theta\Delta t\, L)y^{n+1} = (I + (1-\theta)\Delta t\, L)y^n + \Delta t[(1-\theta)g^n + \theta g^{n+1}]. \quad (3)$$

Backward Euler (BE) uses θ = 1. The trapezoidal rule (TR) uses θ = 1/2. The implementation factors the sparse left-hand matrix once per run and reuses it at each step. The benchmark compares these two integrators on a common stencil. Their error tables are separate from the published schemes in Table 2.

In the joint sweep, N and the number of time steps M both take the values 32, 64, 128 and 256. In the time-only sweep, N is fixed at 256 and M doubles from 32 to 2048. Errors in that sweep are measured against a fine-time TR solution on the same spatial grid with M = 65,536. Repeating the reference run with M = 32,768 checks the temporal reference. In the space-only sweep TR uses M = 4,096 while N doubles from 32 to 256. Repeating those runs with M = 8,192 checks how much the time discretization affects the reported spatial errors.

The metric is the maximum absolute displacement error over interior nodes at T = 1. The joint and space-only sweeps use (2) as the reference. The time-only sweep measures error against the fine-time discrete solution, so it estimates the temporal error of the fixed spatial system. The observed rate is again $\log_2(Ec/Ef)$.

4.3 Discrete energy check

The separate energy runs set f = 0 and use N = M = 128. Write $W = Q^{-1}$. Since $WK = bW - D_h$ is symmetric positive definite, a discrete energy for the homogeneous system is

$$E(U,V) = (h/2)[V^{\mathrm{T}}WV + U^{\mathrm{T}}WK\,U]. \quad (4)$$

The semi-discrete energy satisfies dE/dt = −hV$^{\mathrm{T}}$WAV ≤ 0. For TR, the energy change follows the same dissipation identity evaluated at the step midpoint and multiplied by Δt. For BE, the corresponding endpoint identity contains the additional term −E($U^{n+1} - U^n$, $V^{n+1} - V^n$). Thus both methods have nonincreasing unforced energy for this stencil and positive nodal coefficients. The calculation does not extend automatically to flux-form discretizations, nonhomogeneous boundaries, or forced runs.

5 Benchmark results

Figure 1 and Table 3 show the joint sweep. TR consistently approaches order two. The variable-coefficient BE error increases between the first two grids even though the energy test shows no growth. At N = M = 32, the BE error relative to a fine-time solution on the same spatial grid is 1.396×10^{-3}. The fine-time solution differs from the exact solution by 1.745×10^{-3}, but the total error is only 3.502×10^{-4}. The two error contributions partly cancel on that grid. At N = M = 256 the variable-coefficient BE and TR errors are 2.188×10^{-4} and 2.888×10^{-5}, respectively.

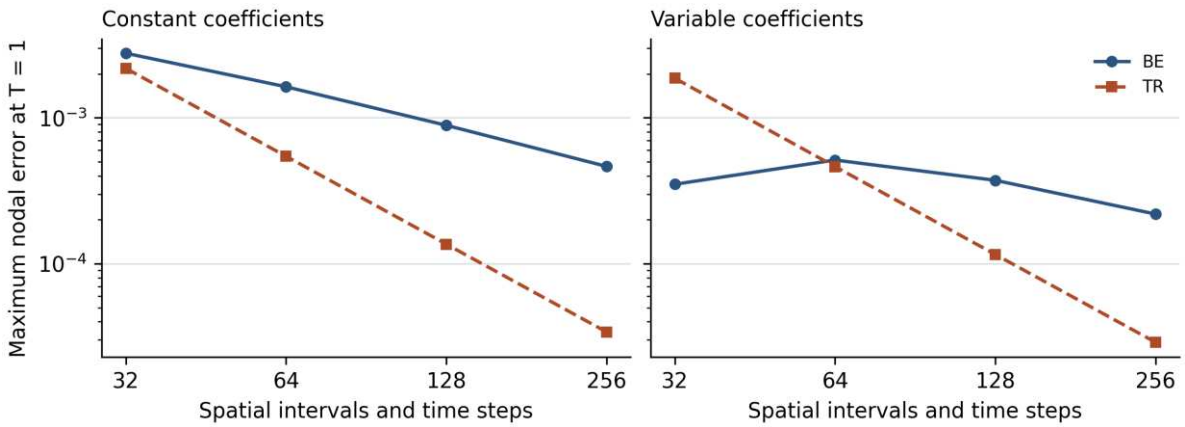


Figure 1 Final-time errors under joint spatial and temporal refinement

Table 3 Final-time maximum errors and observed orders in the joint sweep

N = M	Constant BE Error / order	Constant TR Error / order	Variable BE Error / order	Variable TR Error / order
32	2.770×10^{-3} —	2.183×10^{-3} —	3.502×10^{-4} —	1.867×10^{-3} —
64	1.631×10^{-3} 0.764	5.445×10^{-4} 2.004	5.132×10^{-4} −0.551	4.629×10^{-4} 2.012
128	8.878×10^{-4} 0.878	1.360×10^{-4} 2.001	3.727×10^{-4} 0.462	1.156×10^{-4} 2.002
256	4.641×10^{-4} 0.936	3.401×10^{-5} 2.000	2.188×10^{-4} 0.769	2.888×10^{-5} 2.001

The finest pairs in Table 4 clarify the joint results. The trapezoidal spatial and temporal orders

are close to two in both coefficient cases. The last time-only BE rates are about one, including the variable-coefficient case. The independently refined sweeps distinguish a coarse-grid cancellation effect from the fine-grid behaviour of an integrator.

5.1 Separate refinement and energy results

Table 4 Errors and observed orders at the finest separate refinement pair

Coefficients	Sweep and method	Coarse error	Fine error	Order
Constant	Time BE	1.223×10^{-4}	6.101×10^{-5}	1.003
Constant	Time TR	1.537×10^{-7}	3.840×10^{-8}	2.001
Constant	Space TR	1.263×10^{-4}	3.158×10^{-5}	2.000
Variable	Time BE	6.035×10^{-5}	3.088×10^{-5}	0.966
Variable	Time TR	1.068×10^{-7}	2.669×10^{-8}	2.001
Variable	Space TR	1.088×10^{-4}	2.719×10^{-5}	2.000

The last time refinement doubles M from 1024 to 2048 on N = 256. The last space refinement doubles N from 128 to 256 on M = 4096. The two fine-time reference solutions differ by at most 1.123×10^{-10} in maximum norm. In the space sweep, halving the time step changes the numerical solution by at most 0.023% of the reported error.

Every recorded step decreases the discrete energy in the unforced runs (Table 5). BE dissipates more energy over the interval than TR in these tests, consistent with the extra dissipation term in its energy identity. The energy measurements establish decay for the tested runs, while the forced experiments provide the accuracy comparison.

Table 5 Discrete energy in unforced tests with 128 intervals and time steps

Coefficients	Method	Initial energy	Final energy	Final / initial	Largest step change divided by initial energy
Constant	BE	3.30698	1.82228	0.5510	-6.287×10^{-4}
Constant	TR	3.30698	2.02941	0.6137	-2.064×10^{-4}
Variable	BE	3.22428	1.60840	0.4988	-6.500×10^{-4}
Variable	TR	3.22428	1.82235	0.5652	-1.783×10^{-4}

6 Discussion

The strongest conclusion from the published comparisons is that increasing the formal order reduced error for their smooth constant-coefficient examples [4, 10]. The new results extend the comparison to a particular smoothly varying coefficient profile using a different pair of schemes. They also show how a single coarse-grid result could give the wrong impression about

finer-grid performance. Reporting joint refinement alongside changes in space and time separately puts that result in context.

The benchmark uses one manufactured solution, Dirichlet boundaries, a final-time nodal maximum, and a single smooth coefficient profile. It gives no estimates for discontinuous coefficients, fractional models, Neumann boundaries, or larger domains. Those problems require their own reference solutions and metrics. The review does not pool errors across papers because reported norms, test problems and computational conditions differ. Runtime and memory rankings would require comparable implementations and measured costs.

7 Conclusions

For smooth classical telegraph problems, second-order finite differences provide a useful baseline. The four published constant-coefficient examples recover the expected refinement orders. In the independent benchmark, the trapezoidal rule with a centred spatial stencil gives nearly second-order convergence under separate spatial and temporal refinement for both coefficient profiles. Backward Euler approaches first order in time. Its small error on one coarse variable-coefficient grid results from partial cancellation and does not persist under refinement.

Future comparisons can use the manufactured solution and refinement protocol here as a common starting point. Adding mixed boundary conditions, coefficient interfaces and specified fractional derivatives would test how far the conclusions carry. Error at shared observation times, stability conditions, and computational cost at a specified accuracy would make comparisons across method families more informative.

Declarations

Data and code availability The numerical inputs are defined in the manuscript. The accompanying supplement contains the Python implementation and the generated convergence, diagnostic and energy data. The published error values used in Table 2 are available in [4, 10].

Ethics approval and consent The study uses mathematical models, synthetic numerical data and published papers. No human participants or animals were involved.

Funding No funding received.

Competing interests Authors declares no conflict of interest..

References

[1] R. K. Mohanty (2009). New unconditionally stable difference schemes for the solution of multi-dimensional telegraphic equations. *International Journal of Computer Mathematics*, 86(12), 2061–2071. 10.1080/00207160801965271

[2] M. E. Koksal (2011). An operator-difference method for telegraph equations arising in transmission lines. *Discrete Dynamics in Nature and Society*, 2011, 561015. 10.1155/2011/561015

[3] A. Ashyralyev and M. Modanli (2015). An operator method for telegraph partial differential and difference equations. *Boundary Value Problems*, 2015, 41. 10.1186/s13661-015-0302-z

[4] B. Faraj and M. Modanli (2017). Using difference scheme method for the numerical solution of telegraph partial differential equation. *Journal of Garmian University*, 4 (ICBS Conference), 157–163. 10.24271/garmian.133

[5] F. Ureña, L. Gavete, J. J. Benito, A. García and A. M. Vargas (2020). Solving the telegraph equation in 2-D and 3-D using generalized finite difference method (GFDM). *Engineering Analysis with Boundary Elements*, 112, 13–24. 10.1016/j.enganabound.2019.11.010

[6] M. Dehghan and A. Shokri (2008). A numerical method for solving the hyperbolic telegraph equation. *Numerical Methods for Partial Differential Equations*, 24(4), 1080–1093. 10.1002/num.20306

[7] R. C. Mittal and R. Bhatia (2014). A collocation method for numerical solution of hyperbolic telegraph equation with Neumann boundary conditions. *International Journal of Computational Mathematics*, 2014, 526814. 10.1155/2014/526814

[8] F. Wang and E. Hou (2020). A direct meshless method for solving two-dimensional second-order hyperbolic telegraph equations. *Journal of Mathematics*, 2020, 8832197. 10.1155/2020/8832197

[9] B. Pekmen and M. Tezer (2012). Differential quadrature solution of hyperbolic telegraph equation. *Journal of Applied Mathematics*, 2012, 924765. 10.1155/2012/924765

[10] M. Modanli, B. M. Faraj and F. W. Ahmed (2020). Using matrix stability for variable telegraph partial differential equation. *An International Journal of Optimization and Control: Theories & Applications*, 10(2), 237–243. 10.11121/ijocta.01.2020.00870

[11] R. Jiwari, S. Pandit and R. C. Mittal (2012). A differential quadrature algorithm to solve the two dimensional linear hyperbolic telegraph equation with Dirichlet and Neumann boundary conditions. *Applied Mathematics and Computation*, 218(13), 7279–7294. 10.1016/j.amc.2012.01.006

[12] R. C. Mittal and S. Dahiya (2017). Numerical simulation of three-dimensional telegraphic equation using cubic B-spline differential quadrature method. *Applied Mathematics and Computation*, 313, 442–452. 10.1016/j.amc.2017.06.015

[13] E. Hesameddini and E. Asadolahifard (2016). A new spectral Galerkin method for solving the two dimensional hyperbolic telegraph equation. *Computers & Mathematics with Applications*, 72(8), 1926–1942. 10.1016/j.camwa.2016.08.003

[14] Y. Zhou and Z. Luo (2018). A Crank–Nicolson collocation spectral method for the two-dimensional telegraph equations. *Journal of Inequalities and Applications*, 2018, 137. 10.1186/s13660-018-1728-5

[15] B. Hussain, M. Faheem and A. Khan (2024). A numerical technique based on Legendre wavelet for linear and nonlinear hyperbolic telegraph equation. *Journal of Applied Mathematics and Computing*, 70, 3661–3684. 10.1007/s12190-024-02098-0

[16] S. M. Sayed, A. S. Mohamed, E. M. Abo-Eldahab and Y. H. Youssri (2025). Spectral framework using modified shifted Chebyshev polynomials of the third-kind for numerical solutions of one- and two-dimensional hyperbolic telegraph equations. *Boundary Value Problems*, 2025, 7. 10.1186/s13661-024-01987-4

[17] A. S. Mohamed (2026). Comparative analysis of solution methods for the telegraph equation: differential transform, reduced differential transform, and second-kind Chebyshev collocation techniques. *Advances in Continuous and Discrete Models*, 2026, 76. 10.1186/s13662-026-04123-x

[18] M. Modanlı (2018). Two numerical methods for fractional partial differential equation with nonlocal boundary value problem. *Advances in Difference Equations*, 2018, 333. 10.1186/s13662-018-1789-2

[19] Sh. Baharlouei and R. Mokhtari (2023). A stable and convergent hybridized discontinuous Galerkin method for time-fractional telegraph equations. *Numerical Functional Analysis and Optimization*, 44(11), 1175–1193. 10.1080/01630563.2023.2236690

[20] Kamran, F. Ali Shah, K. Shah and T. Abdeljawad (2025). Numerical solution of two dimensional time-fractional telegraph equation using Chebyshev spectral collocation method. *Partial Differential Equations in Applied Mathematics*, 13, 101129. 10.1016/j.padiff.2025.101129

[21] A. Akgül and B. M. Faraj (2021). Difference scheme method for the numerical solution of partial differential equations. *Transactions in Mathematical and Computational Sciences*, 1(2), 12–22. 10.52587/TMCS010202

[22] M. E. Köksal (2023). Recent developments of numerical methods for analyzing telegraph equations. *Archives of Computational Methods in Engineering*, 30(6), 3509–3527. 10.1007/s11831-023-09909-w

[23] P. Spiteri and F. Messine (2025). Numerical schemes for the solution of the telegrapher equation. *Numerical Algorithms*, 100, 1715–1738. 10.1007/s11075-025-02099-5

[24] M. Asif, F. Bilal, N. Haider and F. Jarad (2025). Robust numerical techniques for modeling telegraph equations in multi-scale and heterogeneous environments. *Journal of Applied Mathematics and Computing*, 71, 6585–6620. 10.1007/s12190-025-02551-8